Journal of University of Duhok, Vol. 20,No.1 (Pure and Eng. Sciences), Pp 626-637, 2017
eISSN: 2521-4861 & pISSN: 1812-7568
https://doi.org/10.26682/sjuod.2017.20.1.55

SIDE WEIR FLOW INVESTIGATION IN A CIRCULAR CHANNEL USING COMPUTATIONAL FLUID DYNAMICS (CFD) FOR SUBCRITICAL FLOW CONDITION

Dr. JOWHAR **R**. **M**OHAMMED and **S**HAMIRAN **J**. **S**HIBA
Dep. of Water Resources Engineering, College of Engineering, University of Duhok, Kurdistan Region-Iraq

ABSTRACT

The 3D flow over side weirs is investigated using Computational Fluid Dynamic (CFD). The study aims to assess the capability of ANSYS CFX code for modeling flow characteristics in a circular channel with side weir for subcritical flow condition. Twelve models were studied for some ranges of variables such as discharge, length and height of side weir. The numerical simulation was based on the solution of continuity and momentum equations for three dimensional, incompressible, steady and turbulent flow. The volume of fluid (VOF) method was used to predict the free surface changes and the RNG k-ε model was employed for simulating the flow field. The experimental data of Uyumaz and Muslu (1985) were used for verification. For all models, the specific energy is obtained and the average energy difference at the upstream and downstream side of the weir was very small and the assumption of constant energy in the circular channel was acceptable. The numerical results predicted the changes in the water surface profile at the main channel central axis and indicated that the water level rises from upstream to downstream end of the weir. The discharge coefficient (C_d) variation with the upstream Froude number (Fr_1) for different weir height and length were studied and it was found that the value of (C_d) decreased with the increase of (Fr_1) value. For each side weir length, the variation of (C_d) with the ratio of the weir height to channel diameter (P/D) were studied and it was observed that with the increase of (P/D) ratio the value of the (C_d) increased. The relation between the (C_d) and the ratio of the side weir length to channel diameter (L/D) for different weir height were also investigated. It was noticed that the (C_d) value increased gradually as the (L/D) ratio increased. The combined effects of (Fr_1), (P/D) and (L/D) on the (C_d) were studied for all models and an empirical expressions for describing this relation was obtained and it was found that (C_d) was a function of all the above parameter.

KEYWORDS: *Subcritical flow, Side weir, Circular channel, turbulence model, VOF model*

1. INTRODUCTION

A side-weir is a lateral outflow structure which is installed into the side of a channel or river to spill or to divert part of water over them when the flow level rises in the channel above the side weir crest level. The flow over side weir represents special case of spatially varying flow (SVF) with decreasing discharge. Side weir is mainly used in sanitary engineering practices and irrigation engineering. Computational Fluid dynamics (CFD) is the process of using numerical methods to provide solution of the governing equations related to flow regime. The recent evolution in the hardware sectors has led to the availability of many CFD packages. These packages give accurate solutions and satisfactory results to many complex problems through numerical modeling. De Marchi (1934) [cited in Mangarulkar (2010)] was one of the earliest researchers who analytically studied flow over rectangular side weirs based on a constant specific energy concept. Many experimental studies have been conducted to find the discharge coefficient equation along the side weir in a rectangular channel [e.g. Hager (1987); Singh *et al.* (1994); Borghei *et al.* (1999)]. Swamee *et al.* (1994) carried out an experimental study in which they obtained the equations for an elementary discharge coefficient for two shapes of side weirs (rectangular and triangular side weirs) constructed in a rectangular channel. The hydraulic characteristics and the discharge coefficient of a triangular side weir in a rectangular channel have been studied by Kumar and Pathak (1987); Ghodsian (2004). Cosars and Agaccioglu (2004) investigated the discharge coefficient of a triangular side weir both on straight and curved channels. Theoretical, experimental and numerical study of flow over side weirs in a circular channel are investigated by Uyumaz and Muslu (1985) and an empirical equation for discharge coefficient of side weir are obtained. Vatantkah (2012) proposed a semi-analytical solution for estimating water

Journal of University of Duhok, Vol. 20,No.1 (Pure and Eng. Sciences), Pp 626-637, 2017
eISSN: 2521-4861 & pISSN: 1812-7568
https://doi.org/10.26682/sjuod.2017.20.1.55

surface profile a long side weir in a circular channel depending on a constant specific energy. Using the energy principles and the finite difference method, Yumaz and Smith (1991) investigated numerically the flow over side weirs in rectangular and circular channels. Mahmodinia *et al.* (2012) used FLUENT program for simulating the free surface flow over side weir and obtained the influence of different Froude number on them. The (CFD) model and the laboratory model were used for obtaining the discharge coefficient of the broad-crested side weir in the trapezoidal channel by Hoseini *et al.* (2013) and the results were in good agreement for both method. Azimi & Shabanlou (2015) used RNG k-ε turbulence models and the volume of fluid (VOF) method to simulate the flow field and flow free surface in a triangular channel along the side weir. Based on the review of the literature a very few numerical simulations were done on a circular channel with side weir for subcritical flow conditions. Accordingly, the present study aims to proposing the numerical simulation for the flow field in a circular channel with a rectangular side weir using the VOF method and RNG k-ε turbulence model, respectively, by CFD code (ANSYS CFX). In continuation, the determination of the discharge coefficient for the side weir is also presented.

2. SIDE WEIR EQUATION

The specific energy in the parent channel should remain constant along the weir length. The specific energy at any section for open channel can be written as (Chow 1959):

$$E = y + \alpha \frac{Q^2}{2gA^2} \qquad (1)$$

where, E is the specific energy, α is a velocity distribution coefficient, y is the flow depth, Q is the main channel discharge, A is the main channel flow area and g is the acceleration due to gravity. Differentiating both sides of Equation (1) with respect to x gives:

$$\frac{dE}{dx} = \frac{dQ}{dx}\left(\alpha \frac{Q}{gA^2}\right) + \frac{dy}{dx}\left(1 - \alpha \frac{Q^2 T}{gA^3}\right) \qquad (2)$$

where, T is the top width of the channel and x is horizontal distance from upstream end of the side weir. Assuming the specific energy is constant along the weir $\left(\frac{dE}{dx} = 0\right)$and solving Equation (2) for $\left(\frac{dy}{dx}\right)$, which is the water surface slope, yields:

$$\frac{dy}{dx} = \frac{\alpha \frac{Q}{gA^2}\left(\frac{dQ}{dx}\right)}{1 - \alpha \frac{Q^2 T}{gA^3}} \qquad (3)$$

Assuming that $S_0 - S_f = 0$ or $S_0 = S_f = 0$ and α=1, the equation of the weir can be written as follow (Chow 1959):

$$q = -\frac{dQ}{dx} = -\frac{2}{3} C_d \sqrt{2g} (y - P)^{3/2} \qquad (4)$$

where, q is the discharge per unit length of the weir, P is weir height and C_d is discharge coefficient. By solving Equation (1) and assuming $\left(\frac{dE}{dx} = 0\right)$, the discharge in the main channel can be obtained as:

$$Q = A\sqrt{2g(E - y)} \qquad (5)$$

where Q is the discharge in the main channel. Knowing the flow depth y and using Equation (5), the discharge over the side weir Q_w, at a distance x from the beginning of the side weir can be determined as:

$$Q_w = Q_1 - Q_2 \qquad (6)$$

where, Q_1 is the discharge at the channel upstream and Q_2 discharge at the channel downstream. By combining Equations (3), (4) and (5), (Uyumaz and Muslu 1985) provided the following equation for discharge per unit length of side weir located in a circular channel:

Journal of University of Duhok, Vol. 20,No.1 (Pure and Eng. Sciences), Pp 626-637, 2017
eISSN: 2521-4861 & pISSN: 1812-7568
https://doi.org/10.26682/sjuod.2017.20.1.55

$$-\frac{dQ_w}{dx} = q = C_d\sqrt{2g(y-P)}(y-P) \qquad (7)$$

Thus the discharge coefficient for side weir is calculated as follows:

$$C_d = \left(\frac{Q_w}{L\sqrt{2g}(y-P)^{3/2}}\right) \qquad (8)$$

where, Q_w is the passing discharge over the side weir.

3. DIMENSIONAL ANALYSIS

Based on Equation (8), the factors affecting the discharge coefficient of a side weir in a circular channel are:

1- Approaching velocity of flow. (v_1)
2- Upstream depth of flow. (y_1)
3- Length and height of side weir. (L and P)
4- Channel diameter. (D)
5- Acceleration due to gravity.(g)

The general relationship for the above variables can be expressed as:

$$C_d = f(V_1, y_1, L, P, D, g) \qquad (9)$$

In this analysis using Buckingham Pi theorem, Equation (9) can be reduced to the form:

$$C_d = f\left(Fr_1, \frac{P}{D}, \frac{L}{D}\right) \qquad (10)$$

where, $Fr_1 = \frac{V_1}{\sqrt{gy_1}}$ is Froude number at the upstream of the side weir.

4. GOVERNING EQUATIONS

CFD is based on the fluid dynamics governing equation and modeling turbulent flow. Most of the commercial software's use the time-averaged modeling equations such as Reynolds-Averaged Navier-Stokes equations (RANS).

The numerical model used in this research is constructed on the time-averaged three-dimensional equations, turbulent, steady and incompressible flow. The Navier-Stokes are the governing equations for an incompressible flow and constant viscosity as expressed below (Piradeepan 2002):

Mass conservation equation

$$\frac{\partial \rho}{\partial t} + \frac{\partial}{\partial x_i}(\rho U_i) = 0 \qquad (11)$$

Momentum conservation equation

$$\frac{\partial(\rho U_i)}{\partial t} + \frac{\partial}{\partial x_j}(\rho U_i U_j) = -\frac{\partial P}{\partial x_i} + \frac{\partial}{\partial x_j}\left[\mu\left(\frac{\partial U_i}{\partial x_j} + \frac{\partial U_j}{\partial x_i}\right)\right] + \frac{\partial}{\partial x_j}\left(-\rho\overline{\acute{u}_i\acute{u}_j}\right) \qquad (12)$$

where,
$\rho =$ fluid density, $t =$ time, $x =$ axis coordinates, $P =$ pressure,
$U_i =$ mean velocity components, μ = dynamic viscosity and $\acute{u}_i =$ fluctuating part of the velocity.

The term ($\frac{-\partial(\rho\overline{\acute{u}_i\acute{u}_j})}{\partial x_j}$) in equation (12) is the Reynolds stresses term. In order to solve the equations system, some form of modeling is required. The turbulence modeling is a computational procedure for finding a closure of the governing equations (Piradeepan 2002).

The Volume of fluid VOF method (Hirt and Nichols 1981) is applied for multiphase flow modeling and this method is ideally used for free surface flow. In this method both the water and the air are not mix together and the interface is moved by introducing the volume fraction. The following continuity equation is solved to calculate the volume component:

$$\frac{\partial \alpha_w}{\partial t} + u_i\frac{\partial \alpha_w}{\partial x_i} = 0 \qquad (13)$$

where,
α_w: the volume fraction of water, t: is time, and u_i: is the velocity in x_i-direction.

The VOF method is based on that the sum of the volume fraction in each control volume is equal to 1, therefore the volume fraction of air can be computed by:

$$\alpha_a = 1 - \alpha_w \qquad (14)$$

The solution of the above equation indicates that, α_w =1 when the element is filled with water, α_w = 0 when the element is totally filled with air and the element contain free water surface when $0 < \alpha_w < 1$.

The RNG k–ε model is used for simulating flow over side weir. This model was derived by (Yakhot and Orszag 1986) by the application of statistical technique (Renormalization Group

Journal of University of Duhok, Vol. 20,No.1 (Pure and Eng. Sciences), Pp 626-637, 2017
eISSN: 2521-4861 & pISSN: 1812-7568
https://doi.org/10.26682/sjuod.2017.20.1.55

method) to the Navier-Stokes equation. The RNG procedure eliminates the small scale of motion from differential equations by expressing their effects in terms of large scale motions and modified viscosity. Additionally the high resolution for Advection Scheme in multiphase simulation and First order Numeric scheme for turbulence kinetic energy are applied.

5. NUMERICAL SIMULATION

5.1 Model Geometry and Mesh Generation

Creating the geometry is the first stage in any CFD model. In this study, the geometry was created using ANSYS design modeler Figure (1). The geometry consists of a horizontal circular channel 5m length, 1m diameter and at one side of the channel the rectangular side weir is installed with different parameters. Twelve models have been generated. In each model, four flow rates were passed. Three different side weir height and four different side weir length were selected for each model

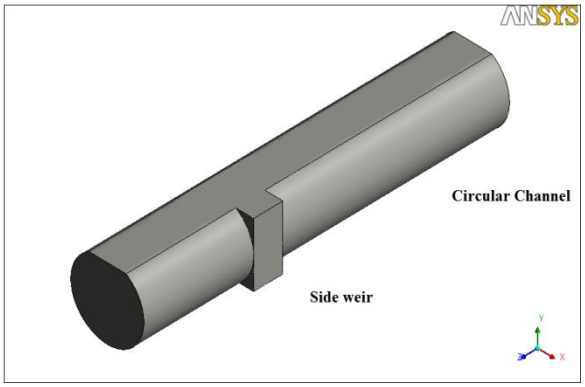

Fig.(1): -The geometry of the circular channel with a side weir.

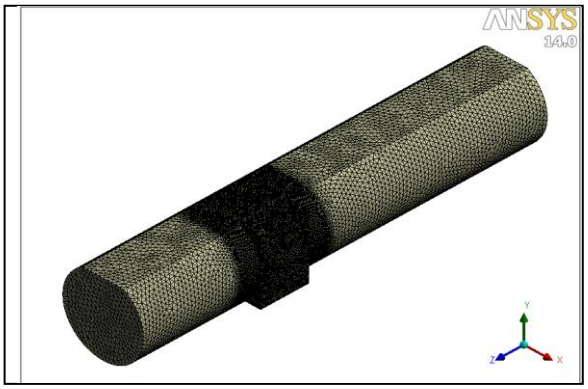

Fig.(2):- 3D and typical view of mesh for circular channel.

In this study, the geometry was divided into three sections and the meshes were built using Automatic method in ANSYS CFX-mesh. The large change of flow phenomena occurs near the side weir, so special care has to be given for meshing side weir. The meshes at the side weir section where finer than the other sections. The type of element was Tetrahedral, as shown in Figures (2) and more details about meshing are given in table (1).

Table (1): Mesh Specification (Tetrahedral element)

Weir height (m)	**0.1**	**0.1**	**0.1**	**0.1**	**0.2**	**0.2**	**0.2**	**0.2**	**0.3**	**0.3**	**0.3**	**0.3**
Weir length (m)	0.3	0.4	0.5	0.6	0.3	0.4	0.5	0.6	0.3	0.4	0.5	0.6
Total number of elements	424,571	449,426	477,929	506,631	420,760	446,247	472,940	501,868	419,162	445,217	471,377	499,855

In locations where there is a large fluctuation in the given variable, the mesh can automatically become finer or coarser. This can be achieved by using a technique called mesh adaption. For the case of free surface flow, the mesh is required to be very fine, Figure (3) shows circular channel with side weir after implementation of the mesh adaption.

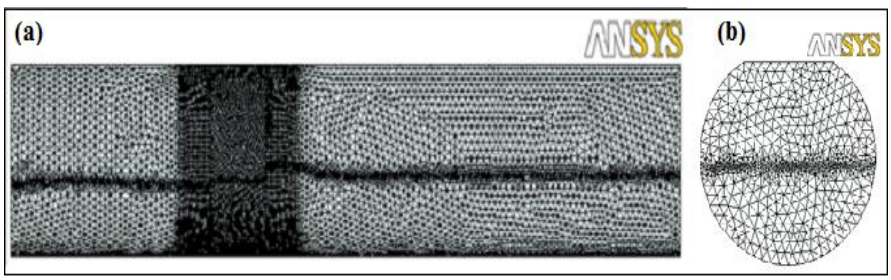

Fig. (3):- Typical mesh adaption technique (a) subcritical flow and (b) inlet region.

Journal of University of Duhok, Vol. 20,No.1 (Pure and Eng. Sciences), Pp 626-637, 2017
eISSN: 2521-4861 & pISSN: 1812-7568
https://doi.org/10.26682/sjuod.2017.20.1.55

5.2 Boundary and Initial Conditions

CEL expressions are used for defining boundary conditions. For the channel inlet the specified amounts of the flow depth and discharge are defined where are for outlet boundary the pressure are defined. Also, the side weir outlet is defined as outlet boundary. For the wall of the circular channel a no slip and a smooth wall were selected for the wall boundaries. Because the present study is the case of free surface flow, the top of the channel is considered as opening with entrainment and zero relative pressure, Figure (4). The initial conditions are Velocity components, upstream pressure and upstream volume fraction of both air and water at the inlet.

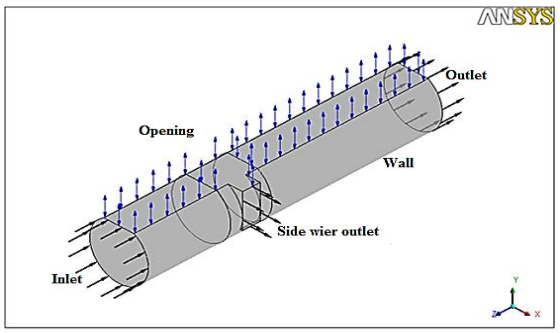

Fig. (4): -The boundary conditions used in the numerical simulation.

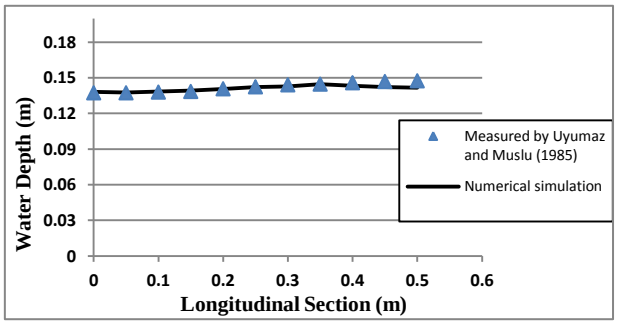

Fig. (5):- Water surface profile comparison along the longitudinal profile.

6. RESULTS AND DISCUSSION

6.1 Verification

In this research, the data of experimental measurements of Uyumaz and Muslu (1985) were used for verifying the numerical model. The experimental work was performed in a horizontal open cannel (S_o=0.0) which include the circular cross section of 0.25m diameter, 10.9m long and a side weir which was placed at the middle section of the main channel, the inlet discharge was 0.017m^3/sec at the main channel, the length and the height of the side weir were L=0.5m and P=0.1m respectively. At the central axis of the main channel the water surface profile for subcritical flow condition were determined. The numerical simulation of the RNG k-ε model was compared with experimental results by plotting experimental data against corresponding simulation results Figure (5). In general, the water surface profile rises from the upstream toward the downstream end of the side weir for subcritical flow condition. The mean absolute percentage error (MAPE) for the flow free surface along the longitudinal profile is defined using equation (15).

$$MAPE = \frac{100}{m}\sum_{i=1}^{m}\left|\frac{observed - predicted}{predicted}\right| \qquad (15)$$

The MAPE value was (1.06) % which shows a good agreement between experimental and numerical modeling.

6.2 Specific Energy

One of the assumptions that have been used to solve the governing equations for discharge over the side weir is the constant specific energy. It is important to examine the validity of this assumption before proceeding to detail analysis. In Figure (6) the specific energy for different discharges in the circular channel at the upstream (E_1) and downstream (E_2) ends of the side weir are compared. The average energy difference at the side weir upstream and downstream is found to be about 1.2%. This shows that the specific energy along the side weir in a circular channel is almost constant. For rectangular channel, Borghi *et al.* (1999) estimated a 3.7% of average energy difference, whereas Azimi and Shabanlou estimated a 5.57% average energy difference for subcritical flow in triangular channel. Thus the assumption of constant energy in a circular channel is acceptable.

Journal of University of Duhok, Vol. 20,No.1 (Pure and Eng. Sciences), Pp 626-637, 2017
eISSN: 2521-4861 & pISSN: 1812-7568
https://doi.org/10.26682/sjuod.2017.20.1.55

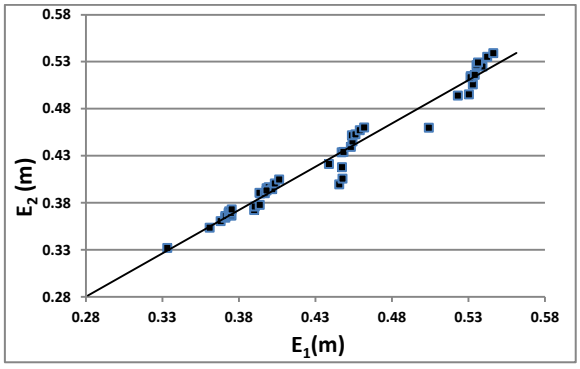

Fig. (6): Comparison of specific energy at the u/s and d/s ends of the side weir.

6.3 Water Surface Profile

To define the flow structure, water surface profiles are obtained along the side weir in the main channel centerline. Figure (7 a-w) shows the longitudinal profiles for various upstream Froude numbers (Fr_1). According to the flows pattern, the behavior of water surface profile will change. For subcritical flow condition, the water depth rises from the upstream end toward the downstream of the side weir and the rate of this rise decreases substantially after the mid span of the side weir crest. In addition to that the side weir height affects the longitudinal water surface profile. It was noticed that for low side weir the water depth has increased at the middle of the side weir to its downstream end, whereas for high side weir the water level rises slightly at the upstream end. The water surface profiles on the other hand depend on the upstream Froude number (Fr_1). It is clear that as the (Fr_1) is increased; the water depth has decreased at the downstream end of the side weir. The same results were obtained for rectangular channel by Mangarulkar (2010), Emiroglu *et al*.(2011) and Mahmodinia *et al*. (2012).

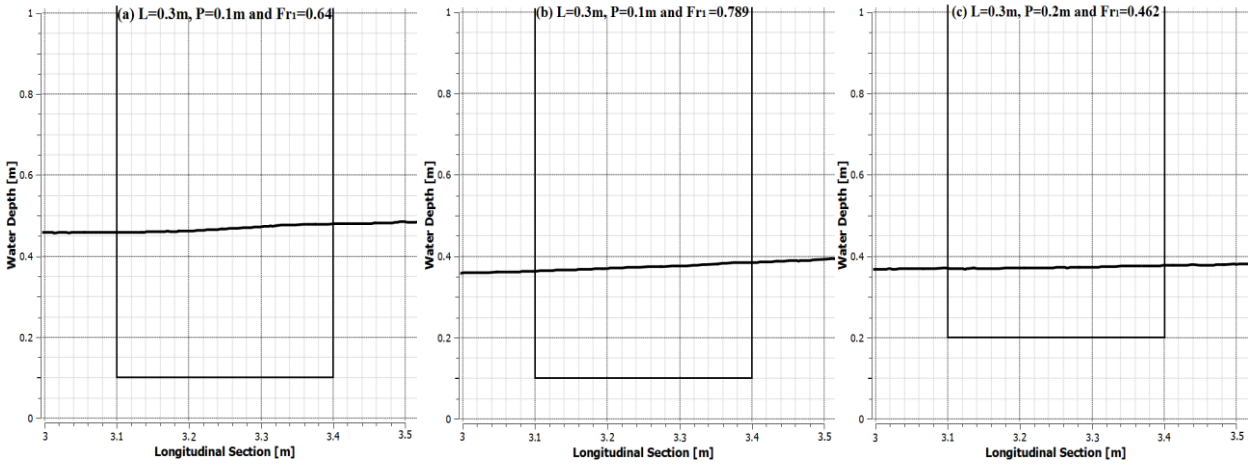

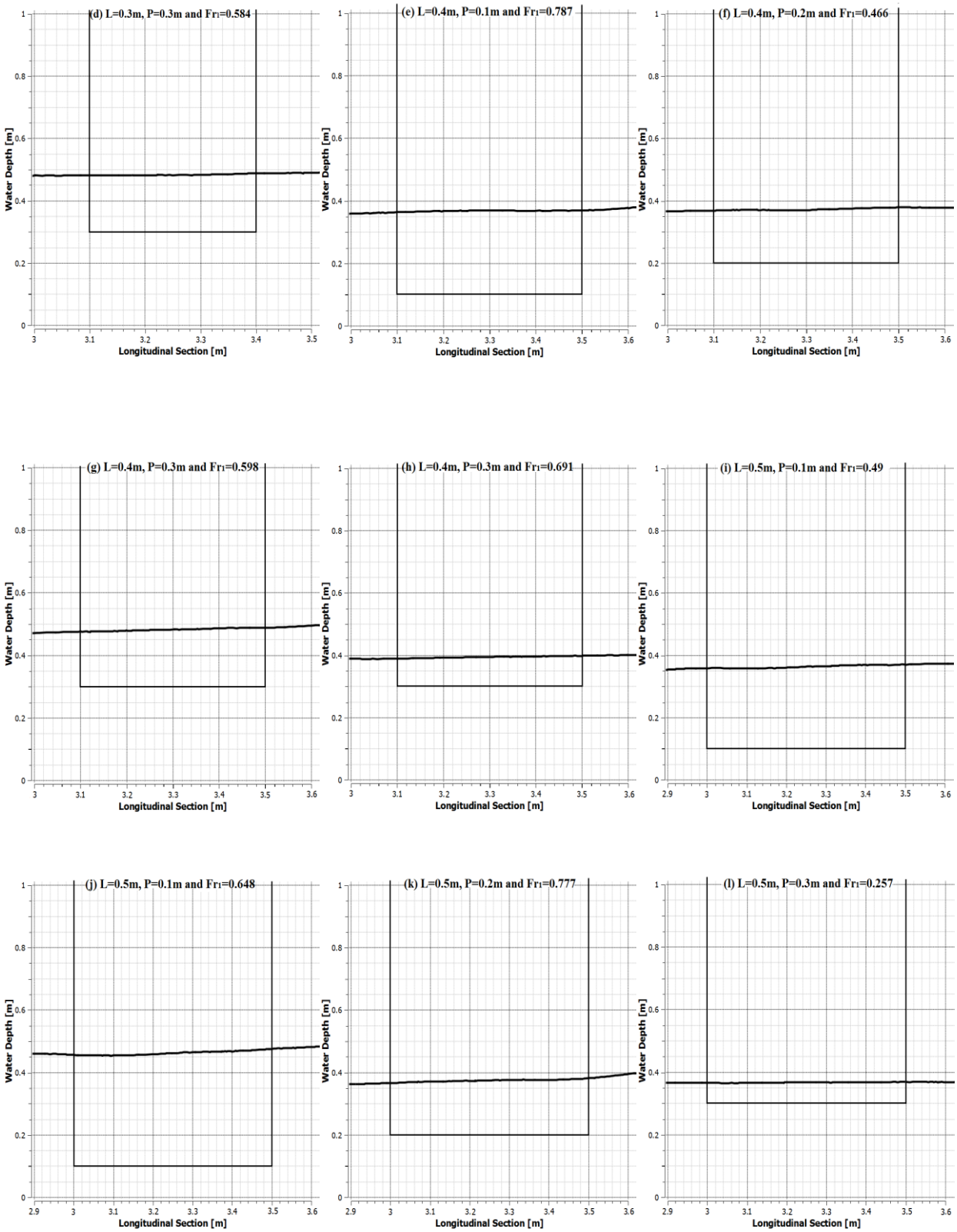
(d) L=0.3m, P=0.3m and Fr1=0.584
(e) L=0.4m, P=0.1m and Fr1=0.787
(f) L=0.4m, P=0.2m and Fr1=0.466
(g) L=0.4m, P=0.3m and Fr1=0.598
(h) L=0.4m, P=0.3m and Fr1=0.691
(i) L=0.5m, P=0.1m and Fr1=0.49
(j) L=0.5m, P=0.1m and Fr1=0.648
(k) L=0.5m, P=0.2m and Fr1=0.777
(l) L=0.5m, P=0.3m and Fr1=0.257
Water Depth [m]
Longitudinal Section [m]

Journal of University of Duhok, Vol. 20,No.1 (Pure and Eng. Sciences), Pp 626-637, 2017
eISSN: 2521-4861 & pISSN: 1812-7568
https://doi.org/10.26682/sjuod.2017.20.1.55

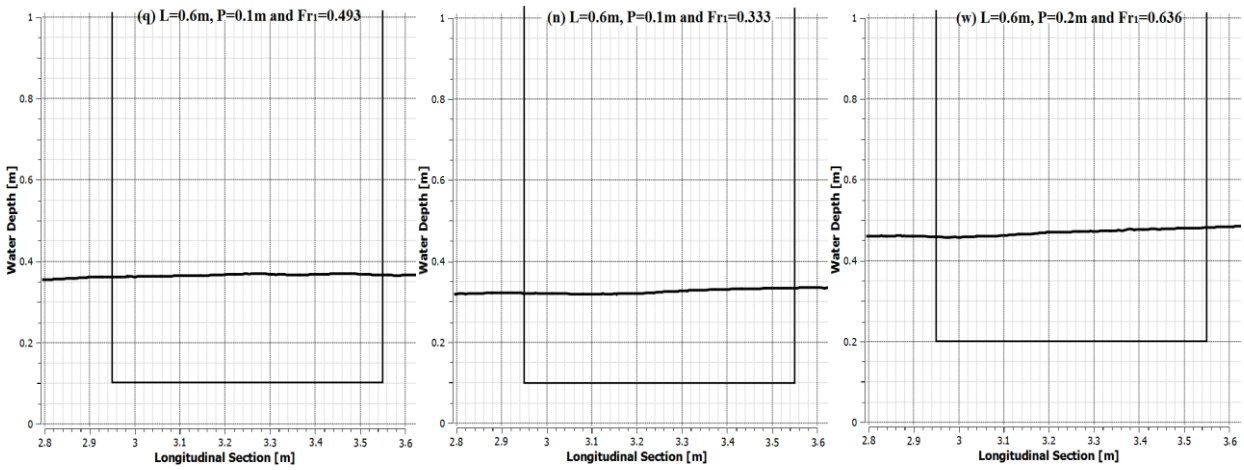

Fig. (7 a-w): Water surface profile along the side weir for different models.

6.4 Data Analysis

6.4.1 Variation of (C_d) with upstream Froude number (Fr_1)

The values of C_d are plotted against the most influencing parameter Fr_1 for different side weir heights. From Figure (8) it was found that C_d reduced with the increase of Fr_1 for subcritical flow. The similar conclusion was reported by Singh *et al* (1994) and Borghei *et al* (1999).

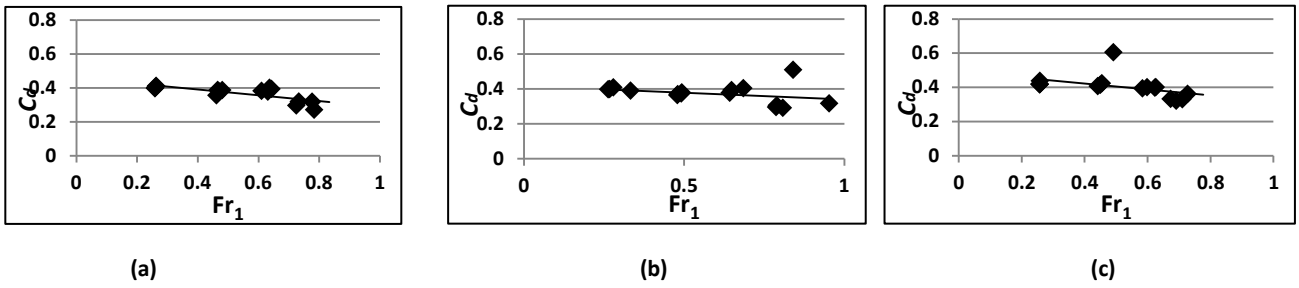

Fig. (8): Variation of *Cd* with Fr_1 for different side weir heights (a) P=0.1m, (b) P=0.2m and (c) P=0.3m.

6.4.2 Variation of (C_d) with the parameter (*P/D*)

Dimensional analysis showed that C_d was dependent on the ratio of side weir height to diameter of circular channel. Figure (9) shows the variation of C_d with (*P/D*) for different side weir lengths. It is obvious that C_d value increases when the (*P/D*) ratio increases.

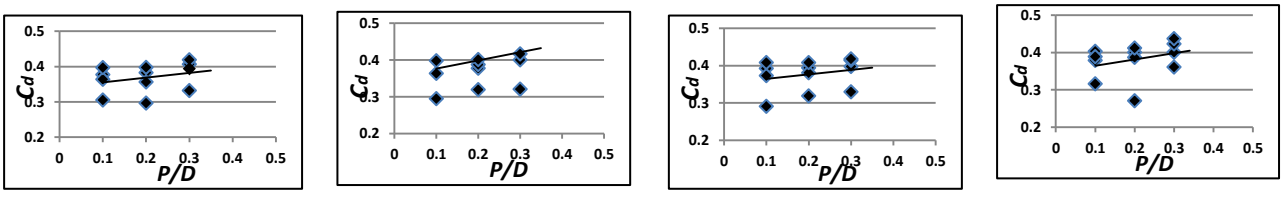

Fig. (9): Variation of *Cd* with *P/D* for different side weir lengths (a) L=0.3m, (b) L=0.4m, (c) L=0.5m and (d) L=0.6m

6.4.3 Variation of (C_d) with the parameter (*L/D*)

Journal of University of Duhok, Vol. 20,No.1 (Pure and Eng. Sciences), Pp 626-637, 2017
eISSN: 2521-4861 & pISSN: 1812-7568
https://doi.org/10.26682/sjuod.2017.20.1.55

The variation of C_d with the ratio of weir length to the circular channel diameter (L/D) was studied for different weir heights as can be seen in Figure (10). The results indicate that C_d value increases gradually with the increase of (L/D).

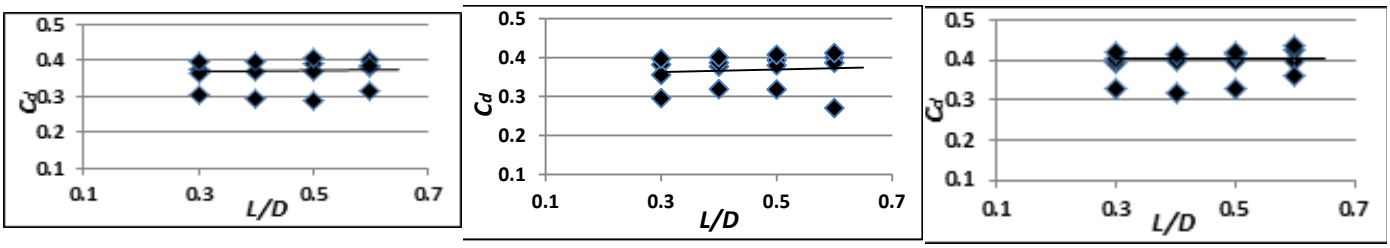

Fig. (10): Variation of *Cd* with *L/D* for different side weir heights (a) P=0.1m, (b) P=0.2m and (c) P=0.3m.

6.4.4 Variation of (C_d) with (Fr_1), (P/D) and (L/D)

In order to study the effect of all no dimensional parameters on C_d, a regression analysis using computer program (SPSS) was used on the data set to obtain an expression of the following form:

$$C_d = -0.860 + 7.745(1 - Fr)^{-0.348} - 6.517\left(\frac{L}{D}\right)^{-0.003} \times (1 - Fr)^{-0.399} + 0.415\left(\frac{P}{D}\right) \times (1 - Fr)^{2.905} \quad (17)$$

Figure (11) shows the relation between C_d predicted by Equation (17) and those observed numerically with the coefficient of determination (R^2 =0.77). They indicate a good agreement between both of them.

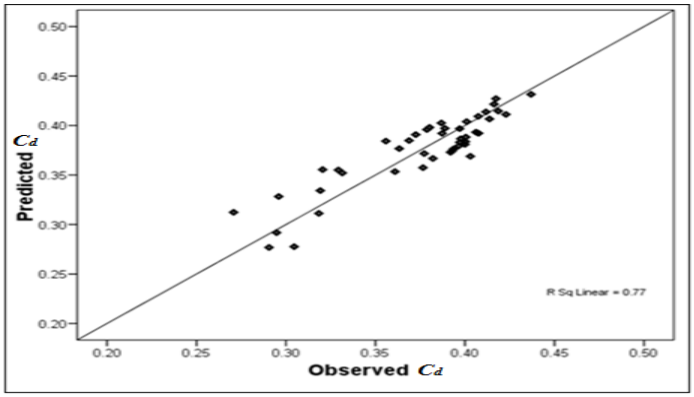

Fig. (11): Variation of observed values of C_d with predicted ones using Equation (17).

5.5 Velocity Contours

The velocity contours have been plotted to identify how the velocity values changes across the channel section. The simulated velocity contour lines for different dimensions of weir are shown in Figure (12). The average velocity increases from the beginning of the side weir towards the middle and then decreases with advances toward downstream end.

Journal of University of Duhok, Vol. 20,No.1 (Pure and Eng. Sciences), Pp 626-637, 2017
eISSN: 2521-4861 & pISSN: 1812-7568
https://doi.org/10.26682/sjuod.2017.20.1.55

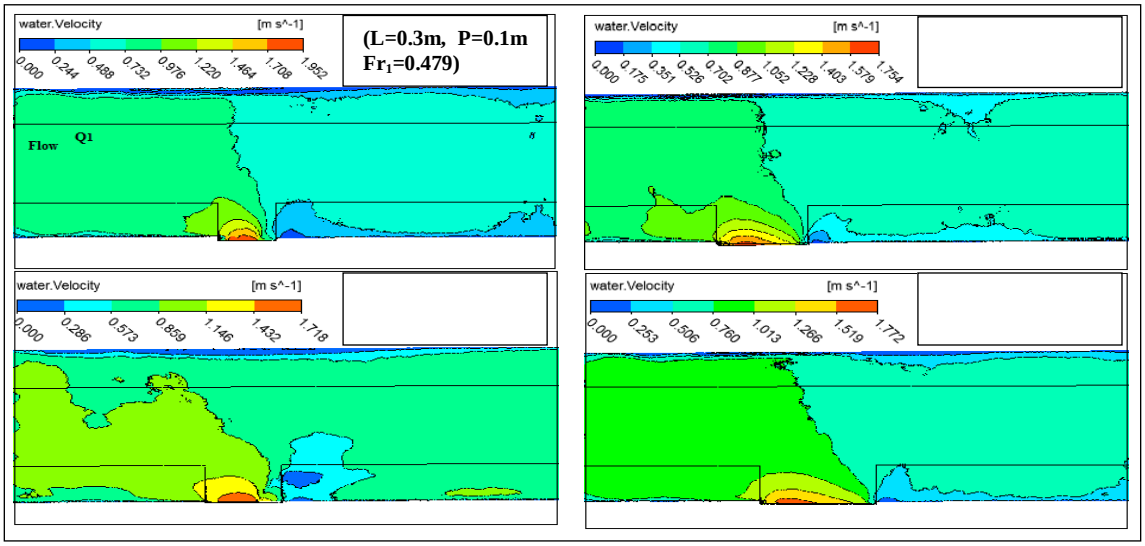

Fig.(12): Water velocity contour for different dimensions of side weir.

5.6 Separation Zone

Separation zone is the region of low velocities and recirculation flow, Figure (13) shows streamline for different upstream Froude number (Fr_1). In Figures (13 a and b) it can be seen that the largest separation zone occurs at the longer crest and there is recirculation inside the separation zone. Also in these figures it is clear that the size and location of the separation zone varies with the Fr_1 value. At low Fr_1 the separation zone occurs opposite to the downstream end of the side weir along the far wall of the channel, but with the increase of Fr_1, the separation zone moves downstream the channel. Figures (13 c and d) show flow streamline for the same model with different Fr_1 values. It can be seen that the separation zone occurs for low value of Fr_1 but, for high Fr_1 the separation zone decreases or does not exists for the same model.

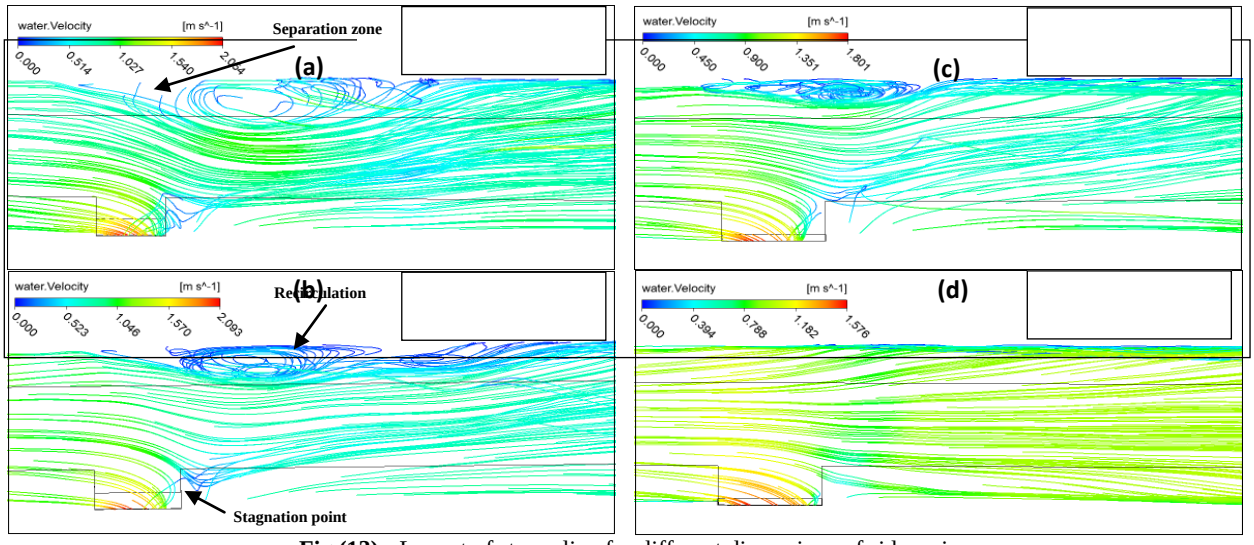

Fig.(13): -Layout of streamline for different dimensions of side weir.

5.7 Dividing Streamline and Stagnation Point

The dividing streamlines and stagnation points within circular channel along the side weir were depicted via velocity vector plots. In Figures (14), (15) and (16) vectors layout at the water surface can be seen. According to the numerical results, the dividing streamline strikes the wall of the main channel near the end of the side weir at the stagnation point and as the Fr_1 increases the stagnation point moves upstream close to the downstream end of the side weir.

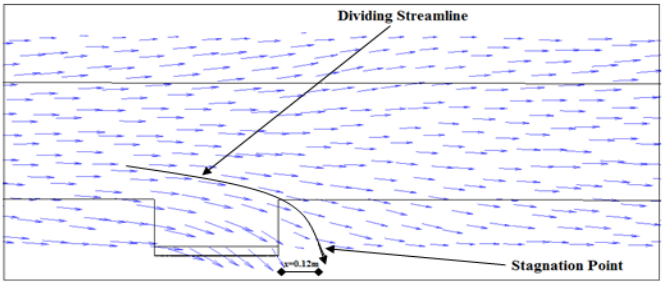

Fig. (14): Velocity vector plot of (L=0.5m), (P=0.3m) and (Fr_1=0.45).

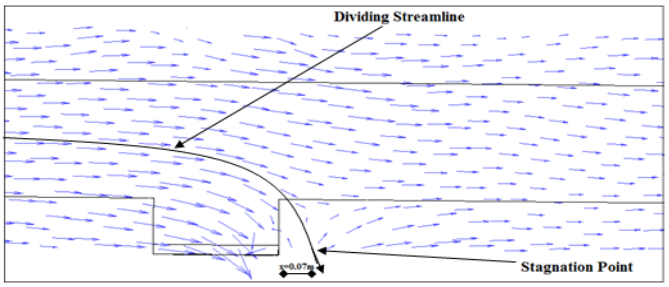

Fig. (15): Velocity vector plot of (L=0.5m), (P=0.3m) and (Fr_1=0.62).

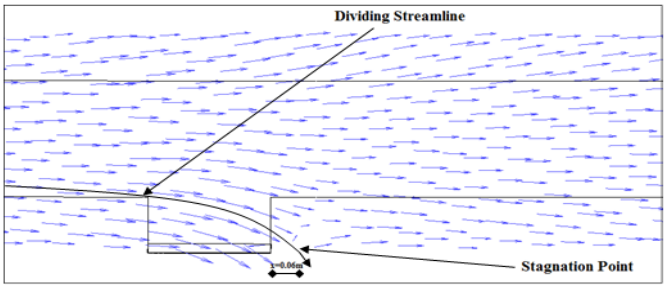

Fig. (16): Velocity vector plot of (L=0.5m), (P=0.3m) and (Fr_1=0.71).

7. CONCLUSIONS

Within the results of the present study, the following findings and conclusions may be drawn:

1. There is a good agreement between the previous experimental and the numerical model results of the free surface flow.
2. The numerical model predicted the changes in the water surface profile at the central axis of the main channel very well and shows that the water level rises from the beginning to the end of the side weir.
3. For all models, the average energy difference at the upstream and downstream of the side weir was very small and the assumption of constant specific energy in the circular channel is acceptable.
4. Applying the finer mesh at the side weir region is very important to assure the reliability of CFD results.
5. The numerical results showed that the size and the location of the separation zone are depended on the Froude number value at the upstream side of the weir and the weir dimensions.
6. In order to study the effect of all dimensionless parameters (Fr_1), (P/D) and (L/D) on (C_d), a regression analysis was used on the data set to obtain an equation between (C_d) and above parameters. The predicted (C_d) by obtain equation and those observed numerically was plotted and showed a good agreement between both of them with the coefficient of determination (R^2 =0.77).

8. REFERENCES

-ANSYS-CFX Help, Release 14.0, (2011): http://www.ANSYS.com.

-Azimi, H. and Shabanlou, S. (2015). The Flow Pattern in Triangular Channels along the Side Weir for Subcritical Flow Regime, Journal of Flow Measurement and Instrumentation 1016-10.

-Borghei, S. M., Jalili, M. R. and Ghodsian, M. (1999). Discharge Coefficient for Sharp-Crested Side Weir in Subcritical Flow, Journal of Irrigation Application and Drainage Engineering, ASCE, Vol. 125, No. 10, PP.1051-1056.

-Chow, V.T., (1959). Open Channel Hydraulics, Mc Graw Hill Boo company, Inc., New York, N.Y.

-Cosar, A. and Agaccioglu, H. (2004). Discharge Coefficient of a Triangular Side-Weir Located on a Curved channel, Journal of Irrigation and Drainage Engineering, ASCE, Vol. 130, No. 5, PP.410-423.

-Ghodsian, M. (2004). Flow over Triangular Side Weir, Journal of Scientia Iranica, Vol. 11, PP.114-120.

Haleem, D. A., Kesserwani, G., and Caviedes-Voullime, D. (2015). Haar waveletbased adaptive finite volume shallow water solver. Journal of Hydroinformatics. Vol. 17(6):857-873

-Hager, W. H. (1987). Lateral Outflow over Side Weirs, Journal of Hydraulic Engineering, Vol. 113, No. 4, PP.491-504.

-Hirt, C.W. and Nichols, B.D. (1981). Volume of Fluid (VOF) Method for the Dynamics of Free Boundaries, Journal of Computational Physics, Vol. 39, No. 1, pp. (201-225).

-Hoseini, S. H., Jahromi, S. H. M., Vahid, M. S. R. (2013). Determination of Discharge Coefficient of Rectangular Broad-Crested Side Weir in Trapezoidal channel by CFD, International Journal of Hydraulic Engineering, Vol. 2, No. 4, PP.64-70.

-Kumar, C. P., and Pathak, S. K. (1987). Triangular Side Weir, Journal of irrigation and Drainage Engineering , ASCE, Vol. 113, No. 1, PP.98-105.

-Mahmodinia, S., Javan, M. and Eghbalzadeh, A. (2012). The Effects of the Upstream Froude Number on the Free Surface Flow over the Side Weirs, Procedia Engineering Journal, Vol. 28, PP.644-647, Avialable online at www.sciencedirect.com .

-Mangarulkar, K. (2010). Experimental and Numerical Study of the Characteristics of Side Weir Flows, M.Sc. Thesis, Department of Building, Civil and Environmental engineering, Concorida University, Canada, http://spectrum.Library.concorida.ca.

-Piradeepan, N. (2002). An Experimental and Numerical Investigation of a Turbulent Airfoil Wake in a 90° Curved Duct, Ph.D. Thesis, Department of Mechanic Engineering, Brunel University.

-Singh, R., Manivannan, D. and satyanarayana, T. (1994). Discharge Coefficient of Rectangular Side Weirs, Journal of Irrigation and Drainage Engineering, ASCE, Vol. 120, No. 4, PP.733-814.

-Swamee, P. K., Pathak, S. K. and Ali, M. S. (1994). Side-Weir Analysis Using Elementary Discharge Coefficient, Journal of Irrigation and Drainage Engineering, Vol. 120, No. 4, PP.742-755.

-Vatankhah, A. R. (2012). A New Solution Method for Water Surface Profile along a Side Weir in a Circular Channel, Journal of Irrigation and Drainage Engineering, ASCE, 1061-10.

-Yakhot, V. and Orszag, S.A. (1986). Renormalization Group Analysis of Turbulence, J. Sci. Comput., Vol. 1, No. 3.

-Uyumaz, A. and Muslu, Y. (1985). Flow over Side Weirs in Circular Channel, Journal of Hydraulic Engineering, Vol. 111, No. 1, PP.144-160.